Optimizing the Open Pit-to-Underground Mining Transition

Barry King[a], Marcos Goycoolea[b], A. Newman[c,*]

[a]*Colorado School of Mines, Operations Research with Engineering (ORwE) PhD Program, Golden, Colorado, 80401, USA*
[b]*Universidad Adolfo Ibañez, School of Business, Peñalolén, Santiago, 7941169, Chile*
[c]*Colorado School of Mines, Mechanical Engineering Department, Golden, Colorado, 80401, USA*

Abstract

A large number of metal deposits are initially extracted via surface methods, but then transition underground without necessarily ceasing to operate above ground. Currently, most mine operators schedule the open pit and underground operations independently and then merge the two, creating a myopic solution. We present a methodology to maximize the NPV for an entire metal deposit by determining the spatial expanse and production quantities of both the open pit and underground mines while adhering to operational production and processing constraints. By taking advantage of a new linear programming solution algorithm and using an ad-hoc branch-and-bound scheme, we solve real-world scenarios of our transition model to near optimality in a few hours, where such scenarios were otherwise completely intractable. The decision of where and when to transition changes the net present value of the mine by hundreds of millions of dollars.

Keywords: Mining/metals industries: optimal extraction sequence; production scheduling: transition problem; integer programming applications: exact and heuristic approaches

1. Introduction and Literature Review

The mining industry contributes trillions of dollars annually to the global economy by providing minerals, metals, and aggregates. This, and volatile metal prices, make it critical that mines possess an efficient production schedule, which can be categorized as: (i) short-term (days to months), (ii) long-term (years), and (iii) strategic (life-of-mine) (Gershon, 1983). A short-term schedule might determine what material to process on a given day; a long-term schedule may examine production rate changes (Epstein et al., 2014; Alonso-Ayuso et al., 2015). Finally, a strategic schedule is used to evaluate large capital investments, and

*Corresponding author: anewman@mines.edu

other decisions that have long-ranging impacts. Because the transition from open pit to underground extraction affects a mine for the remainder of its operational life, it falls into the category of strategic scheduling.

At the time of this writing, a large number of metal deposits are being extracted via surface methods, but plan to transition to concurrently or exclusively extracting ore via underground mining methods. For safety reasons, the underground mine must be sufficiently geographically separated, with horizontally positioned in situ rock, from the open pit mine via what is typically referred to as a crown pillar. Current industry practice places the crown pillar based on: (i) largest economically viable open pit mine, or (ii) the extraction method that results in the largest undiscounted profit for each three-dimensional discretization of the ore body and surrounding rock. Mine operators tend to delay the transition, leading to NPV losses of up to hundreds of millions of dollars. We provide a systematic means by which a mine operator can determine the highest value of a combined open pit and underground design.

The most common method used to extract material is open pit, or surface, mining. Open pit mines vary in both shape and size, and their design is based on the deposit's block model, a model which discretizes the orebody and surrounding rock, and assigns a series of attributes, including mining cost, degree of mineralization (referred to as grade), location, and the cost or profit associated with processing the specific block. Blocks can be categorized using a minimum cutoff grade; blocks at or above the cutoff grade are sent to the processing plant, referred to as a mill, while those below the cutoff grade are sent to a waste dump. The slope angle for the open pit mine, resulting from geotechnical constraints of the host rock, ensures the stability of the pit's walls (Crawford and Hustrulid, 1979).

Given the block attributes and slope angle, mine planners determine the largest economically viable pit for a given deposit, i.e., the ultimate pit limit (Lerchs and Grossman, 1965; Underwood and Tolwinski, 1998). However, while the solution to the ultimate pit limit problem yields the size of the open pit mine, it provides no indication of the extraction sequence required to maximize its discounted value. Johnson (1968) originally formulated the open pit block sequencing problem as an integer program that schedules the extraction of blocks such that the open pit's value is maximized subject to resource and precedence constraints.

Solution techniques for open pit block sequencing problems are still widely studied (Ramazan, 2007; Osanlo et al., 2008; Souza et al., 2010; Topal and Ramazan, 2010; Chicoisne et al., 2012; Shishvan and

Sattarvand, 2015). One such recent significant advance for the linear programming relaxation of a general version of the so-called precedence constrained production scheduling problem (PCPSP), i.e., the open pit block sequencing problem, is with the use of an algorithm outlined in Bienstock and Zuckerberg (2010), which exploits the problem structure (Muñoz et al., 2015). Lambert et al. (2014) present a guide to formulating and efficiently solving monolithic instances of the open pit block sequencing problem, i.e, without decomposition.

Underground mining is used when an economically viable deposit is situated sufficiently deep such that open pit mining is cost prohibitive. There exist many underground mining techniques: (i) open stoping (Figure 1), (ii) room-and-pillar, (iii) sublevel caving, (iv) drift-and-fill, (v) longwall, and (vi) block caving. Determining which method(s) to use is typically based on geotechnical constraints, size, and shape of the deposit (Qinglin et al., 1996). For the purpose of this paper, we confine our discussion to open stoping mining and its associated sequencing options.

A stope is a large, three-dimensional, mineable volume whose maximum size is correlated with the geotechnical properties of the host rock, and is the basic unit for stoping methods. The void left by an extracted stope is sometimes filled with an aggregate to provide structural stability, a process referred to as backfilling. Most underground stoping mines are separated into vertically spaced levels based on the maximum stope height, creating a near-regular grid of possible stope positions (Alford, 2006).

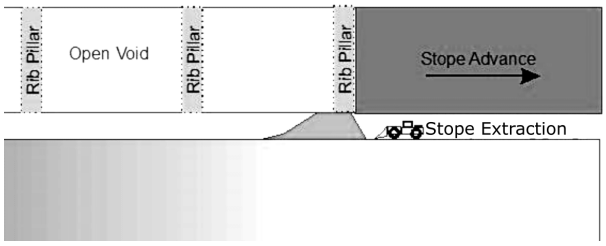

Figure 1: (Open Stoping) In this mining method, rib pillars provide stability, as does the backfilling of open voids left by extracted stopes. Stope advance shows the direction in which mining proceeds.

After determining possible locations from which the ore can economically be extracted, i.e., possible stope locations, mine planners design the development (Alford, 2007; Brazil and Thomas, 2007), which is required to gain access to the ore, provide haulage routes, and maintain proper ventilation within the underground mine. All stoping activities require the completion of a specific set of development activities before

that stope's extraction can commence. Underground sequencing constraints are created after the design, and provide rules for the order in which the development and stopes are extracted. Given a fixed design and sequencing method, we can schedule the underground mining activities to, e.g., maximize NPV, or minimize deviation from production targets (Carlyle and Eaves, 2001; Newman and Kuchta, 2007; Martinez and Newman, 2011; Brickey, 2015; O'Sullivan and Newman, 2015). Trout (1997) provides one of the first generalized formulations for underground stope scheduling; our formulation is a bit more streamlined than his in that we do not differentiate between scheduled and actual decisions, and because we assume that once an activity commences, it must continue at a prescribed rate until finished. The latter characteristic implies that our model contains no continuous variables. On the other hand, we determine sill pillar placement, i.e., locations in which material is left in situ to allow for a change in mining direction, which adds a layer of complexity.

An early transition model assigns large aggregated blocks to be extracted via open pit or underground mining methods in order to maximize value of the deposit (Bakhtavar et al., 2008). This idea was later improved to include the time element and to capture underground capital costs (Newman et al., 2013). In both previous transition models, there is little differentiation between the mining units used above and below ground. The mining industry comments on the difficulty of modeling the transition correctly (Finch, 2012); however, decisions regarding the transition are becoming increasingly relevant (Araneda, 2015). Figure 2 shows an open pit atop an underground mine. The transition zone is depicted as the material that would be extracted were it done via underground methods; the corresponding amount of material would greater were open pit methods used in the transition zone.

We present a new model and corresponding solution techniques to determine the timing of a transition from open pit to underground mining in both a spatial and a temporal sense. This transition incorporates a crown pillar placement that separates the open pit from the underground mine, and of the sill pillars, i.e., levels left in situ that can grant earlier access to stopes by creating a false bottom. Our methodology is based on an ad-hoc branch-and-bound approach that incorporates decomposition methods for solving PCPSP linear programming relaxations, and that includes rounding heuristics. We outline underlying models for the transition in Section 2. Mathematical reformulations to enhance tractability are presented in Section 3, and the solution strategy in Section 4. Sections 5 and 6 provide the numerical results and conclusions,

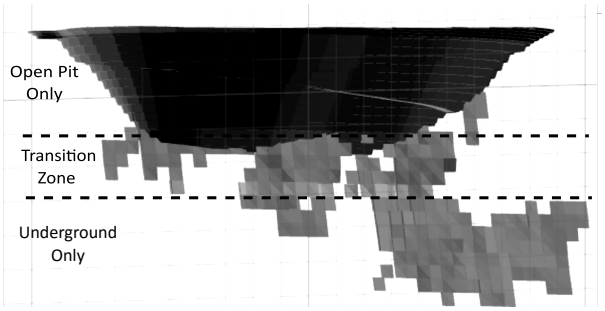

Figure 2: (Transition Zone) The transition zone is an area where it is economically viable to extract material via open pit or underground mining methods. We see the open pit, black, encroaching on the underground mine, gray, in the transition zone.

respectively.

2. Underlying Models

In this section, we introduce three models that underlie our computationally tractable transition model. We first present a surface extraction formulation, followed by an underground formulation, and conclude with a preliminary transition formulation which is essentially a combination of the two.

2.1. Surface Model

We consider a surface model based on open pit mining with a multi-phase pit design (Figure 3), in which a phase corresponds to a sub-region of the pit. A block within a phase consists of all of the material in the phase that resides within a predefined vertical distance. (Note that some mine operators refer to our blocks as benches.) Inside each block, there exists a series of bins that are differentiated by grade, categorized as waste, low, medium, or high, and geological properties. This type phase-block-bin scheduling is common in the mining industry and is the basis for the Minemax (2013) software package. Whittle Consulting (2013) have developed multiple products for this type of scheduling.

The objective of the surface model, ($\mathbb{S}$), is to schedule the extraction, stockpiling, and mill feed in such a way that the NPV is maximized, while adhering to annual extraction and milling capacity constraints. In addition, the desired shape of the open pit is maintained by precedence constraints, which can be categorized into two types: (i) intra-phase precedence expresses that the blocks inside the phase be extracted from the surface down and (ii) inter-phase precedence expresses that blocks inside a phase be extracted only after a specific block in the predecessor phase has been fully extracted. A maximum sinking rate restricts the

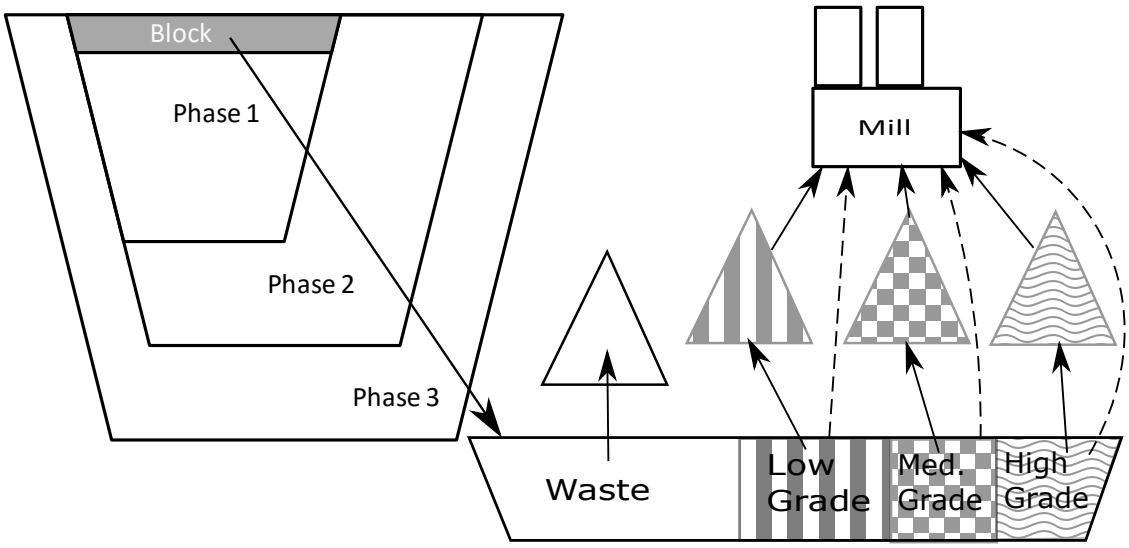

Figure 3: (Phase-block-bin Data Aggregation) The phases are shown as sub-pits with a block occupying a small vertical space within the phase. Each block is separated into bins based on grade. Material in the low- (stripes), medium- (checkered), and high- (waves) grade bins may go directly to the mill (dashed arrows), or to an individual stockpile (solid arrows). Waste is sent to the dump. Although naturally occurring material of different grades is scattered within the block, for stylistic purposes, we group material of each grade.

number of blocks in each phase one can mine in a given time period based on operating constraints. We also require that the material contained in each block and bin be extracted in equal proportion to prevent selective extraction within the block. Once extracted, individual bins can be directed to one of three destinations: waste dump, stockpile, or mill. All material that is below cutoff grade is sent to the waste dump.

Stockpiling is important in our application, because processing stockpiled material augments the underground production to ensure that the mill remains at maximum capacity after extraction ceases in the open pit mine. Bley et al. (2012) outline the formulation from which we construct our "warehouse-style" stockpiling strategy, i.e., each stockpile contains only one block-bin combination; the objective function value corresponding to an optimal solution subscribing to this strategy provides an upper bound on the NPV that can be obtained. Material retrieved from the stockpile is identical to material placed in the stockpile. Some authors have attempted to use "mixing constraints" to more accurately model the characteristics of material retrieved from a stockpile (Bley et al., 2012), but Moreno (2016) show that there are both more accurate and more tractable methods for modeling inventory; they also show that the warehouse model indeed provides a reasonable approximation of reality, within a few percentage points of the "real" net present value for rep-

resentative data sets (not unlike our own). For ease of exposition and to enable us to use a special solution strategy, we omit rehandling costs from our formulations. For our transition model, these costs prove to be insignificant; post-processing them into the objective function value results in hundredths of a percentage change, an amount that is not likely to significantly increase were we to impose the rehandling costs a priori and certainly not sufficiently substantial to consider as part of strategic planning costs.

We define the notation below. In general, use of lower case letters is reserved for indices and parameters. Upper case letters in Roman font represent variables, and sets are given in calligraphic font. An $\mathbb{S}$ superscript on a parameter or variable denotes notation specific to the surface model; we use hats to differentiate parameters and variables that represent similar entities.

Indices and sets:

$b \in \mathcal{B}$	blocks b
$n \in \mathcal{N}_b$	bins in block b
$\hat{b} \in \hat{\mathcal{B}}_b$	blocks that must be mined directly before block b
$b \in \mathcal{B}_p$	blocks in phase p
$d \in \mathcal{D}$	bin destination (1 = mill, 2 = stockpile, 3 = waste)
$p \in \mathcal{P}$	phases p
$r \in \mathcal{R}$	resources (1 = mine, 2 = mill, 3 = sinking rate)
$t \in \mathcal{T}$	time periods

Data:

$c^{\mathbb{S}-}_{nb}$	mining cost for bin n in block b [\$]
$c^{\mathbb{S}+}_{nb}$	revenue generated after having milled bin n of block b [\$]
$q^{\mathbb{S}}_{rnb}$	quantity of resource r consumed by bin n of block b [1 & 2 = tonnes]
$\underline{r}_{rt}, \bar{r}_{rt}$	minimum, maximum amount of resource r available in time t [1 & 2 = tonnes, 3 = blocks]
δ_t	discount factor for time period t (fraction)

Decision variables:

$X^{\mathbb{S}}_{bt}$	1 if block b has finished being extracted by the end of time t; 0 otherwise
$Y^{\mathbb{S}}_{nbdt}$	fraction of bin n in block b extracted by the end of time t and sent to destination d
$I^{\mathbb{S}}_{nbt}$	fraction of bin n from block b in the stockpile at the end of time t
$I^{\mathbb{S}-}_{nbt}$	fraction of bin n from block b sent to the mill from stockpile at the beginning of time t

$$(\mathbb{S}) \quad \max \quad \sum_{b\in\mathcal{B}}\sum_{n\in\mathcal{N}_b}\sum_{t\in\mathcal{T}} \delta_t c^{\mathbb{S}+}_{nb}((Y^{\mathbb{S}}_{nb1t} - Y^{\mathbb{S}}_{nb1,t-1}) + I^{\mathbb{S}-}_{nbt}) - \sum_{b\in\mathcal{B}}\sum_{n\in\mathcal{N}_b}\sum_{d\in\mathcal{D}}\sum_{t\in\mathcal{T}} c^{\mathbb{S}-}_{nb}(Y^{\mathbb{S}}_{nbdt} - Y^{\mathbb{S}}_{nbd,t-1}) \tag{1a}$$

$$\text{s.t.} \quad \sum_{d\in\mathcal{D}} Y^{\mathbb{S}}_{nbd,t-1} \le \sum_{d\in\mathcal{D}} Y^{\mathbb{S}}_{nbdt} \quad \forall b \in \mathcal{B}, n \in \mathcal{N}_b, t \in \mathcal{T} \tag{1b}$$

$$X^{\mathbb{S}}_{b,t-1} \le X^{\mathbb{S}}_{bt} \quad \forall b \in \mathcal{B}, t \in \mathcal{T} \tag{1c}$$

$$\sum_{d\in\mathcal{D}} Y^{\mathbb{S}}_{n-1,bdt} = \sum_{d\in\mathcal{D}} Y^{\mathbb{S}}_{nbdt} \quad \forall b \in \mathcal{B}, n \in \mathcal{N}_b, t \in \mathcal{T} \tag{1d}$$

$$X^{\mathbb{S}}_{bt} \le \sum_{d\in\mathcal{D}} Y^{\mathbb{S}}_{nbdt} \quad \forall b \in \mathcal{B}, n \in \mathcal{N}_b, t \in \mathcal{T} \tag{1e}$$

$$\sum_{d\in\mathcal{D}} Y^{\mathbb{S}}_{nbdt} \le X^{\mathbb{S}}_{\hat{b}t} \quad \forall b \in \mathcal{B}, n \in \mathcal{N}_b, \hat{b} \in \hat{\mathcal{B}}_b, t \in \mathcal{T} \tag{1f}$$

$$I^{\mathbb{S}}_{nb,t+1} = I^{\mathbb{S}}_{nbt} - I^{\mathbb{S}-}_{nbt} + (Y^{\mathbb{S}}_{nb2t} - Y^{\mathbb{S}}_{nb2,t-1}) \quad \forall b \in \mathcal{B}, n \in \mathcal{N}_b, t \in \mathcal{T} \tag{1g}$$

$$\underline{r}_{rt} \le \sum_{b\in\mathcal{B}}\sum_{n\in\mathcal{N}_b}\sum_{d\in\mathcal{D}} q^{\mathbb{S}}_{rnb}(Y^{\mathbb{S}}_{nbdt} - Y^{\mathbb{S}}_{nbd,t-1}) \le \bar{r}_{rt} \quad \forall r \in \mathcal{R} \ni r = 1, t \in \mathcal{T} \tag{1h}$$

$$\underline{r}_{rt} \le \sum_{b\in\mathcal{B}}\sum_{n\in\mathcal{N}_b} q^{\mathbb{S}}_{rnb}((Y^{\mathbb{S}}_{nb1t} - Y^{\mathbb{S}}_{nb1,t-1}) + I^{\mathbb{S}-}_{nbt}) \le \bar{r}_{rt} \quad \forall r \in \mathcal{R} \ni r = 2, t \in \mathcal{T} \tag{1i}$$

$$\sum_{b\in B_p} (X^{\mathbb{S}}_{bt} - X^{\mathbb{S}}_{b,t-1}) \le \bar{r}_{rt} \quad \forall p \in \mathcal{P}, r \in \mathcal{R} \ni r = 3, t \in \mathcal{T} \tag{1j}$$

$$0 \le Y^{\mathbb{S}}_{nbdt}, I^{\mathbb{S}}_{nbt}, I^{\mathbb{S}-}_{nbt} \le 1; X^{\mathbb{S}}_{bt} \text{ binary} \quad \forall b \in \mathcal{B}, n \in \mathcal{N}_b, d \in \mathcal{D}, t \in \mathcal{T} \tag{1k}$$

The objective (1a) maximizes discounted revenue associated with mill profits, and mining costs. Constraints (1b) and (1c) ensure that once a bin-block combination is completed, it remains completed. Constraints (1d) preclude selective mining of any bin in a block, i.e., the constraint forces all bins to be mined in equal proportion. Constraints (1e) relate the fractional and binary extraction variables. Constraints (1f) enforce precedence by preventing the extraction of a block until its predecessors' blocks have been fully extracted. Constraints (1g) balance the inventory in the stockpile at the end of every time period. Constraints (1h) limit the capacity for extraction tonnes in each time period. Constraints (1i) bound processing at the mill in each time period. Constraints (1j) prevent mining too rapidly in one phase. Constraints (1k) enforce nonnegativity and integrality of the decision variables, as appropriate.

2.2. Underground Model

Our underground formulation incorporates a mine design based on pre-constructed stope shapes, organized into vertical levels. Drifts, i.e., tunnels that are only open at one end, are used to access the mine. A vertical decline is a drift that descends from the surface to the lowest underground level. On each level, horizontal drifts are constructed from the decline to the stope locations. Our method sequences stopes from

the bottom up such that extraction and backfilling on the level underneath the given level must be completed before extraction on the given level can begin. The method advances such that mining proceeds away from an initial stope determined a priori. The ore contained within a sill pillar (Figure 4) is partially sterilized and can only be recovered, with significant dilution, at the end of the mine life. Sill pillar placement must balance the sterilization of ore with the increase in net present value gained by earlier access to stopes.

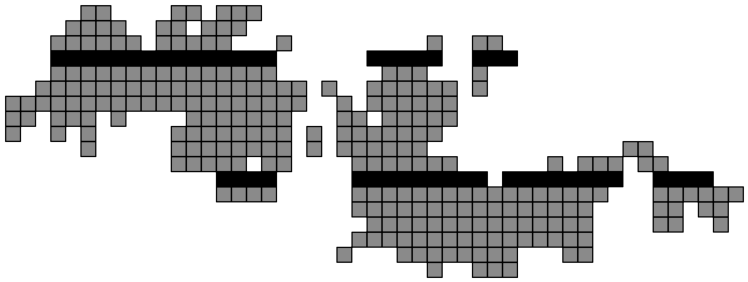

Figure 4: (Regular Grid of Stopes) Sill pillar levels are black, and each block constitutes a designed stope. Any horizontal level of stopes shown in the figure could act as a sill pillar.

The precedence relationships for an underground mine that uses this sequencing method can be categorized as follows: (i) Fixed predecessors include the development required to access the stope, and stopes on the same level. These predecessors ensure that with respect to the mining direction, the adjacent stope on the same level be fully extracted and backfilled before extraction of the next stope can commence. If no adjacent stope on the level exists, then the stope has only development activities as predecessors. (ii) Conditional stope predecessors require that the stope directly below and the stopes on either side of the given stope on the level below must be fully extracted and backfilled before the given stope can be extracted. If the stopes on the level below act as a sill pillar, then the conditional predecessors are omitted (Figure 5). In addition, every underground activity has a set of predecessor activities that are dictated by the mine design.

The underground mine scheduling model, ($\mathbb{U}$), determines sill pillar placement and a life-of-mine schedule consisting of development, stoping, and backfilling activities to maximize the underground mine's NPV. This model precludes specific pairs of activities from being completed in the same time period, and resource constraints limit development, extraction, and backfilling. We assume fixed activity rates.

We maintain the same notation style as in the surface model, but use the superscript $\mathbb{U}$ to represent

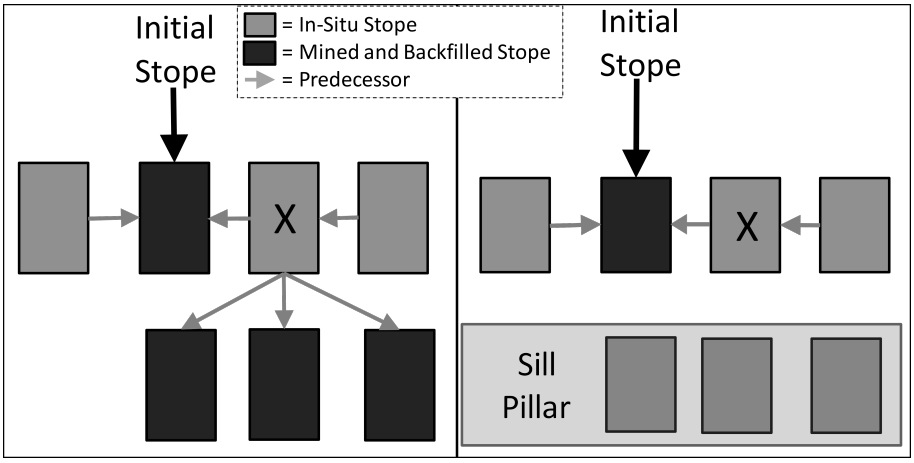

Figure 5: (Sequencing Method) The initial stope location is labeled, with a black arrow, and Stope X's predecessors are denoted by gray arcs. On the left is an example of standard precedence, i.e., both fixed and conditional predecessors. On the right is a stope that has only fixed predecessors, because the sill pillar eliminated all of the conditional predecessors.

underground-specific parameters and variables; we use checks and bars as accents.

Indices and sets:

$a \in \mathcal{A}$	set of all activities
$s \in \mathcal{S} \subset \mathcal{A}$	set of stoping activities
$\check{a} \in \check{\mathcal{A}}_a$	set of fixed predecessors for activity a
$\bar{a} \in \bar{\mathcal{A}}_a$	set of fixed predecessor activities $\bar{a}$ that must be completed one time period in advance of activity a
$\check{s} \in \check{\mathcal{S}}_s \subset \check{\mathcal{A}}_s$	set of conditional predecessors $\check{s}$ below stope s
$\bar{s} \in \bar{\mathcal{S}}_s \subset \bar{\mathcal{A}}_s$	set of conditional predecessor stopes $\bar{s}$ that must be completed one or more time periods in advance of stope s
$l \in \mathcal{L}$	levels in the mine
$l \in \check{\mathcal{L}}_s$	level on which stope s exists (set has cardinality of one)
$r \in \mathcal{R}$	resources (4 = mine/mill capacity, 5 = backfill capacity, 6 = development capacity)

Data:

$c_a^{\mathbb{U}}$	monetary value associated with completing activity a [\$]
$q_{ra}^{\mathbb{U}}$	quantity of resource r associated with activity a [2, 4 & 5 = tonnes, 6 = meters]
$\underline{r}_{rt}, \bar{r}_{rt}$	minimum, maximum level of resource r in time t [4–5 = Mtonnes/yr, 6 =m/yr]
δ_t	discount factor for time period t (fraction)

Decision variables:

$X_{at}^{\mathbb{U}}$	1 if activity a is finished by the end of time t; 0 otherwise
$W_l^{\mathbb{U}}$	1 if level l serves as a sill pillar; 0 otherwise

$$(\mathbb{U}) \quad \max \quad \sum_{a \in \mathcal{A}} \sum_{t \in \mathcal{T}} \delta_t c_a^{\mathbb{U}} (X_{at}^{\mathbb{U}} - X_{a,t-1}^{\mathbb{U}}) \tag{2a}$$

$$\text{s.t.} \quad X_{a,t-1}^{\mathbb{U}} \leq X_{at}^{\mathbb{U}} \quad \forall\, a \in \mathcal{A}, t \in \mathcal{T} \tag{2b}$$

$$X^{\mathbb{U}}_{at} \le X^{\mathbb{U}}_{\check{a}t} \quad \forall\, a \in \mathcal{A}, \check{a} \in \check{\mathcal{A}}_a, t \in \mathcal{T} \tag{2c}$$

$$X^{\mathbb{U}}_{st} \le X^{\mathbb{U}}_{\check{s}t} + W^{\mathbb{U}}_{l} \quad \forall\, s \in \mathcal{S}, \check{s} \in \check{S}_s, l \in \check{\mathcal{L}}_{\check{s}}, t \in \mathcal{T} \tag{2d}$$

$$X^{\mathbb{U}}_{at} \le X^{\mathbb{U}}_{\bar{a},t-1} \quad \forall\, a \in \mathcal{A}, \bar{a} \in \bar{\mathcal{A}}_a, t \in \mathcal{T} \tag{2e}$$

$$X^{\mathbb{U}}_{st} \le X^{\mathbb{U}}_{\bar{s},t-1} + \sum_{i \le j \le k} W^{\mathbb{U}}_{j} \quad \forall\, s \in \mathcal{S}, \bar{s} \in \bar{S}_s, i \in \check{\mathcal{L}}_{\bar{s}}, k \in \check{\mathcal{L}}_s, t \in \mathcal{T} \tag{2f}$$

$$X^{\mathbb{U}}_{st} + W^{\mathbb{U}}_{l} \le 1 \quad \forall\, s \in \mathcal{S}, l \in \check{\mathcal{L}}_s, t \in \mathcal{T} \tag{2g}$$

$$\underline{r}_{rt} \le \sum_{a \in \mathcal{A}} q^{\mathbb{U}}_{ra}(X^{\mathbb{U}}_{at} - X^{\mathbb{U}}_{a,t-1}) \le \bar{r}_{rt} \quad \forall\, r \in \mathcal{R} \ni r \ge 4, t \in \mathcal{T} \tag{2h}$$

$$X^{\mathbb{U}}_{at}, W^{\mathbb{U}}_{l} \text{ binary} \;\; \forall a \in \mathcal{A}, l \in \mathcal{L}, t \in \mathcal{T} \tag{2i}$$

The objective function (2a) maximizes net present value. Constraints (2b) ensure that once an activity is completed, it remains completed. Constraints (2c) enforce fixed precedence, and constraints (2d) enforce conditional precedence based on sill pillar placement. Constraints (2e) ensure that at least one time period elapses between the completion of the specified pair of activities. Constraints (2f) force at least one time period to elapse between the completion of two given stoping activities unless a sill pillar exists on a level inbetween them; these stoping activities need not be on consecutive levels because the precedence might actually allow stopes on consecutive levels to be mined in the same time period. Constraints (2g) prevent mining the stopes on level l, if level l acts as a sill pillar. Constraints (2h) bound extraction, backfill, and development resource use. (Mill processing capacity is essentially unconstrained underground because of the low production rate.) All variables are required to be binary by (2i).

Delay constraints, (2e) and (2f), capture sub-annual detail in our model with annual time fidelity, and exclude two specified activities (a', a) from being completed in the same time period, where a' is a predecessor of a, and the minimum time required to elapse between the start of a' and the completion of a is greater than the time fidelity of the model. It is important to construct a minimal number of delay constraints so as not to unnecessarily increase the number of precedence constraints.

2.3. Basic Transition Model

The basic transition model, ($\mathbb{T}^b$), may be formulated by combining of the surface, ($\mathbb{S}$), and underground, ($\mathbb{U}$), models. The objective function maximizes the NPV of the combined open pit and underground operations, i.e., the sum of (1a) and (2a). A vast majority of the constraints, (1b)-(1h), (1j), (1k), and (2b)-(2i), remain the same as in their respective models. The precedence constraints in both the open pit and un-

derground mine do not need to be changed based on the crown pillar location, because of the direction of extraction for each method. Any non-zero lower bounds on the underground mine's resource constraints are removed to allow for a delayed start of the underground mine. The resource constraints must be altered to accurately reflect that the open pit, stockpile, and/or underground mine may be sending material to the mill in the same time period. Constraints associated with the additional variables, i.e., that represent the crown pillar location, preclude any open pit or underground extraction of material located in the crown pillar. Additional notation is shown below with the superscript $\mathbb{T}^b$ representing transition model-specific variables.

Indices and sets:

$v \in \mathcal{V}$ set of crown pillar elevations

$\tilde{b} \in \tilde{\mathcal{B}}_v$ set of blocks that exist below the crown pillar if the crown pillar is located at elevation v

$\tilde{a} \in \tilde{\mathcal{A}}_v$ set of activities that exist above the crown pillar if the crown pillar is located at elevation v

Decision variables:

$W_v^{\mathbb{T}^b}$ 1 if the crown pillar is located a elevation v; 0 otherwise

$$(\mathbb{T}^b) \quad \max \quad \sum_{b\in\mathcal{B}}\sum_{n\in\mathcal{N}_b}\sum_{t\in\mathcal{T}} \delta_t c_{nb}^{\mathbb{S}+}((Y_{nb1t}^{\mathbb{S}} - Y_{nb1,t-1}^{\mathbb{S}}) + I_{nbt}^{\mathbb{S}-}) - \sum_{b\in\mathcal{B}}\sum_{n\in\mathcal{N}_b}\sum_{d\in\mathcal{D}}\sum_{t\in\mathcal{T}} \delta_t c_{nb}^{\mathbb{S}-}(Y_{nbdt}^{\mathbb{S}} - Y_{nbd,t-1}^{\mathbb{S}})$$
$$+ \sum_{a\in\mathcal{A}}\sum_{t\in\mathcal{T}} \delta_t c_a^{\mathbb{U}}(X_{at}^{\mathbb{U}} - X_{a,t-1}^{\mathbb{U}}) \tag{3a}$$

$$s.t. \quad X_{\tilde{b}t}^{\mathbb{S}} \le 1 - W_v^{\mathbb{T}^b} \quad \forall \tilde{b} \in \tilde{\mathcal{B}}_v, v \in \mathcal{V}, t \in \mathcal{T} \tag{3b}$$

$$X_{\tilde{a}t}^{\mathbb{U}} \le 1 - W_v^{\mathbb{T}^b} \quad \forall \tilde{a} \in \tilde{\mathcal{A}}_v, v \in \mathcal{V}, t \in \mathcal{T} \tag{3c}$$

$$\sum_{v\in\mathcal{V}} W_v^{\mathbb{T}^b} = 1 \tag{3d}$$

$$\underline{r}_{rt} \le \sum_{b\in\mathcal{B}}\sum_{n\in\mathcal{N}_b} q_{rnb}^{\mathbb{S}}((Y_{nb1t}^{\mathbb{S}} - Y_{nb1,t-1}^{\mathbb{S}}) + I_{nbt}^{\mathbb{S}-}) + \sum_{a\in\mathcal{A}} q_{ra}^{\mathbb{U}}(X_{at}^{\mathbb{U}} - X_{a,t-1}^{\mathbb{U}}) \le \bar{r}_{rt} \quad \forall r \in \mathcal{R} \ni r = 2, t \in \mathcal{T} \tag{3e}$$

$$W_v^{\mathbb{T}^b} \text{ binary} \quad \forall v \in \mathcal{V} \tag{3f}$$

Retained constraints from ($\mathbb{S}$): (1b), (1c), (1d), (1e), (1f), (1g), (1h), (1j), (1k)

Retained constraints from ($\mathbb{U}$): (2b), (2c), (2d), (2e), (2f), (2g), (2h), (2i)

The objective function (3a) maximizes net present value of the entire deposit and replaces (1a) and (2a). Constraints (3b) allow for open pit mining to only occur above the crown pillar. Constraints (3c) restrict underground mining to only occur below the crown pillar. Constraint (3d) forces the placement of a crown pillar. Constraints (3e) replace constraints (1i) with respect to mill capacity.

3. Reformulations

The basic transition model, ($\mathbb{T}^b$), is theoretically NP-hard, and, in practice, real-world size problems are intractable with current computer hardware and software. Our scenarios contain nearly 50,000 variables and more than 1.5 million constraints, even after efficient variable elimination techniques are used (Lambert et al., 2014; O'Sullivan, 2013).

Bienstock and Zuckerberg (2010) provide an algorithm, the "BZ algorithm," for efficiently solving the LP relaxation of problems with the math structure seen in PSPCP, i.e., a model in which a majority of the constraints are precedence, rather than "side," e.g., knapsack, constraints. In practice, the BZ algorithm's solution time is more sensitive to the latter type of constraints than to the number of precedence constraints. Muñoz et al. (2015) provide an implementation framework for solving the LP relaxation of open pit mining problems using the BZ algorithm, and show that it is possible to obtain LP relaxation solutions to PCPSPs with millions of variables and precedence constraints, but fewer than 200 "side" constraints, orders of magnitude faster than simplex-based methods. With reformulation and an ad-hoc branch-and-bound strategy, we are able to identify open pit-to-underground transition options with near-optimal NPVs.

We reformulate the basic transition model ($\mathbb{T}^b$) by transforming some of the side constraints into precedence constraints, specifically, a special knapsack, (1j), and the "warehouse-style" inventory, (1g), constraints in the surface model, ($\mathbb{S}$). Mathematical proofs showing that these reformulations are no weaker than the original formulations can be found in the appendix.

3.1. Special Knapsack Reformulations

We show how to transform sinking rate constraints, (1j), into precedence constraints by exploiting the facts that: (i) the blocks within a phase are required to be completed in a fixed order, i.e., blocks must be extracted in sequential order from the surface downwards, and (ii) the left-hand side is 0 for all time periods in all scenarios. Constraints (1j) from the initial surface model ($\mathbb{S}$) appear as follows:

$$\sum_{b \in B_p} (X^{\mathbb{S}}_{bt} - X^{\mathbb{S}}_{b,t-1}) \leq \bar{r}_{rt} \quad \forall p \in \mathcal{P}, r \in \mathcal{R} \ni r = 3, t \in \mathcal{T} \tag{4}$$

The reformulation of constraint (4) prevents a block b that is $\bar{r}_{3t}$ successor blocks away from the selected

block $\tilde{p}$ in the phase from being completed in the same time period as block b. This requires the following set definition:

$\tilde{p} \in \tilde{\mathcal{P}}_b$ predecessors for block b that must be completed at least one time period prior to block b

The reformulation is shown in (5):

$$X^{\mathbb{S}}_{bt} \leq X^{\mathbb{S}}_{\tilde{p},t-1} \quad \forall b \in \mathcal{B}, \tilde{p} \in \tilde{\mathcal{P}}_b, t \in \mathcal{T} \tag{5}$$

This constraint set, (5), has far greater cardinality than (4), but possesses precedence structure. Figure 6 shows an example of the constraint construction.

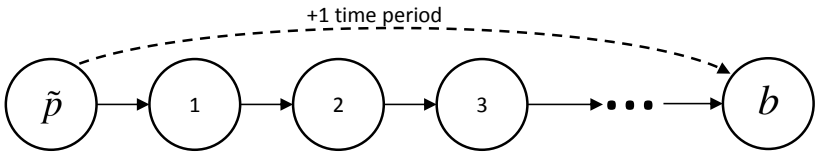

Figure 6: (Special Knapsack Reformulation) An additional precedence arc, dashed, is added to prevent block $\tilde{p}$ and the successor block b from being completed in the same time period, because their precedence separates them by more blocks than can be completed in a time period. Immediate precedence is shown with solid arcs.

3.2. Inventory Balance Reformulations

In this section, we present a reformulation of the inventory balance constraints (1g):

$$I^{\mathbb{S}}_{nb,t+1} = I^{\mathbb{S}}_{nbt} - I^{\mathbb{S}-}_{nbt} + (Y^{\mathbb{S}}_{nb2t} - Y^{\mathbb{S}}_{nb2,t-1}) \quad \forall b \in \mathcal{B}, n \in \mathcal{N}_b, t \in \mathcal{T} \tag{6}$$

Our reformulation implies that material must be placed in inventory before it is processed in the same or in a later time period, and is mathematically equivalent to the original under the assumption that there is no value lost for placing material in inventory, i.e., there is no mixing, degradation, or rehandling cost associated with placing or retrieving material. We require the following variable definitions:

$\hat{Y}^{\mathbb{S}}_{bt}$ fraction of block b extracted and able to be processed by the end of time t
$Z^{\mathbb{S}}_{nbt}$ fraction of bin n in block b sent to the mill by the end of time t

We replace all instances of variables $Y^{\mathbb{S}}_{nbdt}$ with the appropriate $\hat{Y}^{\mathbb{S}}_{bt}$ or $Z^{\mathbb{S}}_{nbt}$ variables, where the former newly introduced variable represents the fraction of a block extracted in time t, without recognizing the destination. The latter newly introduced variable $Z^{\mathbb{S}}_{nbt}$ tracks both the processing time period and destination of each bin-block combination. If both variables for a given bin-block combination assume a value of 1 in the same time period, that bin-block combination is immediately sent to the mill for processing after extraction. For all periods in which a specific bin-block combination is in the stockpile, the variable representing that block's extraction, $\hat{Y}^{\mathbb{S}}_{bt}$, assumes a value of 1 and the corresponding variable representing processing, $Z^{\mathbb{S}}_{nbt}$, assumes a value of 0. Any bin-block combination that is extracted and not processed is sent to the waste dump, resulting in all corresponding $Z^{\mathbb{S}}_{nbt}$ variables possessing a value of 0. The reformulation of (6) is shown in (7):

$$Z^{\mathbb{S}}_{nbt} \leq \hat{Y}^{\mathbb{S}}_{bt} \quad \forall b \in \mathcal{B}, n \in \mathcal{N}_b, t \in \mathcal{T} \tag{7}$$

Constraints (7) allow only material that has been extracted to be sent to the mill. This reformulation also requires substituting the variables $Y^{\mathbb{S}}_{nbdt}$ and $I^{\mathbb{S}-}_{nbt}$ in the objective function and mill capacity constraints with $\hat{Y}^{\mathbb{S}}_{bt}$ and $Z^{\mathbb{S}}_{nbt}$:

$$\max \quad \sum_{b\in\mathcal{B}} \sum_{n\in\mathcal{N}_b} \sum_{t\in\mathcal{T}} \delta_t c^{\mathbb{S}+}_{nb} (Z^{\mathbb{S}}_{nbt} - Z^{\mathbb{S}}_{nb,t-1}) - \sum_{b\in\mathcal{B}} \sum_{n\in\mathcal{N}_b} \sum_{t\in\mathcal{T}} \delta_t c^{\mathbb{S}-}_{nb} (\hat{Y}^{\mathbb{S}}_{bt} - \hat{Y}^{\mathbb{S}}_{b,t-1}) \tag{8}$$

and

$$\underline{r}_{rt} \leq \sum_{b\in\mathcal{B}} \sum_{n\in\mathcal{N}_b} q^{\mathbb{S}}_{rnb} (Z^{\mathbb{S}}_{nbt} - Z^{\mathbb{S}}_{nb,t-1}) \leq \bar{r}_{rt} \quad \forall r \in \mathcal{R} \ni r = 2, t \in \mathcal{T} \tag{9}$$

For all other constraints, the variable $\hat{Y}^{\mathbb{S}}_{bt}$ replaces $Y^{\mathbb{S}}_{nbdt}$; and, the variables $I^{\mathbb{S}}_{nbt}$ and $I^{\mathbb{S}-}_{nbt}$ are eliminated.

3.3. Enhanced Transition Model

The enhanced transition model is the combination of the reformulated surface ($\mathbb{S}$) and underground ($\mathbb{U}$) mine scheduling models, in which the crown and sill pillar placements are fixed a priori. All other constraints are similar to those in the basic transition model, ($\mathbb{T}^b$). The hat and tilde accents are reserved for open pit sets, and bar accents for underground sets. Additional notation and the enhanced transition model ($\mathbb{T}^e$) follow:

Indices and sets:
$\bar{p} \in \bar{\mathcal{P}}_a$ predecessors for activity a that must be completed at least one time period in advance of activity a

$$
\begin{aligned}
(\mathbb{T}^e) \quad \max \quad & \sum_{b\in\mathcal{B}}\sum_{n\in\mathcal{N}_b}\sum_{t\in\mathcal{T}} \delta_t c^{\mathbb{S}+}_{nb}(Z^{\mathbb{S}}_{nbt} - Z^{\mathbb{S}}_{nb,t-1}) - \sum_{b\in\mathcal{B}}\sum_{t\in\mathcal{T}} \delta_t c^{\mathbb{S}-}_{b}(\hat{Y}^{\mathbb{S}}_{bt} - \hat{Y}^{\mathbb{S}}_{b,t-1}) && \text{(10a)}\\
& + \sum_{a\in\mathcal{A}}\sum_{t\in\mathcal{T}} \delta_t c^{\mathbb{U}}_{a}(X^{\mathbb{U}}_{at} - X^{\mathbb{U}}_{a,t-1})\\
\text{s.t.} \quad & X^{\mathbb{S}}_{b,t-1} \le X^{\mathbb{S}}_{bt} \quad \forall b \in \mathcal{B}, t \in \mathcal{T} && \text{(10b)}\\
& \hat{Y}^{\mathbb{S}}_{b,t-1} \le \hat{Y}^{\mathbb{S}}_{bt} \quad \forall b \in \mathcal{B}, t \in \mathcal{T} && \text{(10c)}\\
& Z^{\mathbb{S}}_{nb,t-1} \le Z^{\mathbb{S}}_{nbt} \quad \forall b \in \mathcal{B}, n \in \mathcal{N}_b, t \in \mathcal{T} && \text{(10d)}\\
& X^{\mathbb{U}}_{a,t-1} \le X^{\mathbb{U}}_{at} \quad \forall a \in \mathcal{A}, t \in \mathcal{T} && \text{(10e)}\\
& X^{\mathbb{S}}_{bt} \le \hat{Y}^{\mathbb{S}}_{bt} \quad \forall b \in \mathcal{B}, t \in \mathcal{T} && \text{(10f)}\\
& \hat{Y}^{\mathbb{S}}_{bt} \le X^{\mathbb{S}}_{\hat{b}t} \quad \forall b \in \mathcal{B}, \hat{b} \in \hat{\mathcal{B}}_b, t \in \mathcal{T} && \text{(10g)}\\
& Z^{\mathbb{S}}_{nbt} \le \hat{Y}^{\mathbb{S}}_{bt} \quad \forall b \in \mathcal{B}, n \in \mathcal{N}_b, t \in \mathcal{T} && \text{(10h)}\\
& X^{\mathbb{U}}_{at} \le X^{\mathbb{U}}_{\bar{p}t} \quad \forall a \in \mathcal{A}, \bar{p} \in \bar{\mathcal{P}}_a, t \in \mathcal{T} && \text{(10i)}\\
& \hat{Y}^{\mathbb{S}}_{bt} \le \hat{Y}^{\mathbb{S}}_{\tilde{p},t-1} \quad \forall b \in \mathcal{B}, \tilde{p} \in \tilde{\mathcal{P}}_b, t \in \mathcal{T} && \text{(10j)}\\
& X^{\mathbb{U}}_{at} \le X^{\mathbb{U}}_{\bar{p},t-1} \quad \forall a \in \mathcal{A}, \bar{p} \in \bar{\mathcal{P}}_a, t \in \mathcal{T} && \text{(10k)}\\
& \underline{r}_{rt} \le \sum_{b\in\mathcal{B}}\sum_{n\in\mathcal{N}_b} q^{\mathbb{S}}_{rnb}(\hat{Y}^{\mathbb{S}}_{bt} - \hat{Y}^{\mathbb{S}}_{b,t-1}) \le \bar{r}_{rt} \quad \forall r \in \mathcal{R} \ni r = 1, t \in \mathcal{T} && \text{(10l)}\\
& \underline{r}_{rt} \le \sum_{b\in\mathcal{B}}\sum_{n\in\mathcal{N}_b} q^{\mathbb{S}}_{rnb}(Z^{\mathbb{S}}_{nbt} - Z^{\mathbb{S}}_{nb,t-1}) + \sum_{a\in\mathcal{A}} q^{\mathbb{U}}_{ra}(X^{\mathbb{U}}_{at} - X^{\mathbb{U}}_{a,t-1}) \le \bar{r}_{rt} \quad \forall r \in \mathcal{R} \ni r = 2, t \in \mathcal{T} && \text{(10m)}\\
& \underline{r}_{rt} \le \sum_{a\in\mathcal{A}} q^{\mathbb{U}}_{ra}(X^{\mathbb{U}}_{at} - X^{\mathbb{U}}_{a,t-1}) \le \bar{r}_{rt} \quad \forall r \in \mathcal{R} \ni r \ge 4, t \in \mathcal{T} && \text{(10n)}\\
& X^{\mathbb{U}}_{at}, X^{\mathbb{S}}_{bt} \text{ binary} \quad \forall a \in \mathcal{A}, b \in \mathcal{B}, t \in \mathcal{T} && \text{(10o)}\\
& 0 \le \hat{Y}^{\mathbb{S}}_{bt}, Z^{\mathbb{S}}_{nbt} \le 1 \quad \forall b \in \mathcal{B}, n \in \mathcal{N}_b, t \in \mathcal{T} && \text{(10p)}
\end{aligned}
$$

The objective function (10a) maximizes net present value, and replaces the objective function (3a). Constraints (10b), (10c), (10d), and (10e) ensure that each completed activity or block remains completed, and are a substitute for (1b), (1c), and (2b). Constraints (10f) and (10g) enforce the precedence structure for the open pit mine, and replace (1e) and (1f). Note that the replacement constraints do not sum on the destination

index because all material is sent to a stockpile, even if just instantaneously. Constraints (10h) ensure that the fraction of a bin that is sent to the mill is no greater than the fraction extracted from the corresponding block, and is a reformulation of (1g). Constraint (10i) enforces underground mine precedence, and is used instead of constraints (2c), (2d), and (2g). Constraints (10j) and (10k) ensure that one time period elapses between the completion of two specific activities or blocks, and are a replacement for constraints (1j), (2e), and (2f). Constraint (10l) bounds open pit-specific resource use, and is a substitute for constraints (1h). Constraint (10m) bounds the mill capacity, and is a substitute for constraints (3e). Constraint (10n) bounds underground-specific resource consumption, and is equivalent to constraints (2h). Constraints (10o) and (10p) enforce binary and variable bounds, where appropriate.

4. Solution Strategy

We obtain near-optimal solutions for the enhanced transition model, ($\mathbb{T}^e$), presented in §3.3, by: (i) exhaustively searching possible crown and sill pillar placement options using an ad-hoc branch-and-bound strategy and solving the resulting LP relaxations, (ii) using a rounding heuristic to convert the LP relaxation solutions with favorable objective function values into integer solutions, and (iii) using integer solutions to eliminate a number of possible crown and sill pillar placement options to reduce the amount of computation required in (ii).

The reformulation in Subsections 3.1 and 3.2 reduces the number of side constraints in the basic transition model, ($\mathbb{T}^b$), but the model is still not in the desired form for obtaining an efficient LP relaxation solution using the BZ algorithm. By fixing, i.e., branching on, all of the variables associated with the placement of the crown and sill pillars, $W_l^{\mathbb{U}}$ and $W_v^{\mathbb{T}^b}$, respectively, we convert all of the conditional precedence constraints, (2d) and (2f), in the underground model, ($\mathbb{U}$), to standard precedence constraints, and the basic transition model at each node to a model with a PCPSP mathematical structure. We branch as follows: For each possible crown pillar placement (which, for our data set, is twelve), we consider all sill pillar placements consisting of between zero and three such pillars, where three would be a maximum operationally feasible number. The total number of viable crown and sill pillar placement options numbers in the thousands.

We first solve the LP relaxation of the transition model for each set of reasonable crown and sill pillar placements, i.e., for each branch, using the BZ algorithm. We then sort these LP relaxation solutions,

decreasing by objective function value. Solutions with the best LP relaxation objective function values are transformed into IP solutions using TopoSort (Chicoisne et al., 2012), which has been shown to provide near-optimal solutions quickly for open pit mine scheduling problems that only have non-zero upper bounds on resource constraints, and which is based on the premise that the earlier the expected completion time of a block or activity in the LP solution, the earlier the block or activity is scheduled in the IP solution. The algorithm maintains precedence constraints by the fact that the expected completion time of a block or activity in the LP relaxation is always greater than or equal to that of its predecessors. Also employed in our variant of TopoSort is an "alpha points" procedure in which activities are ordered not by their expected completion time, but by the time period in which a specified fraction, i.e., alpha point, of the activity has been completed. Therefore, an alpha point of 0.7 would set the order based on the first time period in which the "by" variable obtains a value larger than 0.7. The TopoSort heuristic allows for us to match the ($\mathbb{T}^e$) formulation exactly, i.e, create a mixed integer solution to the open pit portion, and a fully integral solution to the underground portion. Once an IP solution is obtained from the LP relaxations with the largest objective function values, we use bound dominance to eliminate a significant number of the crown and sill pillar placement options. Specifically, every LP relaxation whose objective function value is less than that of an existing feasible IP solution's cannot correspond to an optimal integer placement of the crown and sill pillar.

5. Data and Numerical Results

We introduce the data required for the enhanced transition model. Computational results highlight the speed, effectiveness, and robustness of the methodology which yields consistent near-optimal solutions to our multiple scenarios of the transition model.

5.1. Data

Our industry partner provided all of the data required for the transition model from an active mine in Africa; grade and cost data are confidential. The deposit is known to extend over a large vertical expanse, and the overlap between the upper-most designed stope and lowest-planned open pit extraction elevation is over 400 meters; nearly 80% of the remaining recoverable material is located in this overlap, or transition zone.

The open pit dataset consist of a four-phase design for a partially extracted open pit mine with a total of 336 blocks ranging in weight from 20,000 to 5,500,000 tonnes. Blocks may contain a high-, medium-, and low-grade bin for two material types based on processing properties, and a waste bin. This results in a total of 1,312 bin-block combinations ranging from 250 to 1,100,000 tonnes. Extraction activities may possess as many as three immediate predecessor activities. The cost of extraction increases as the depth of the open pit increases. Subsection 2.1 provides a detailed description of the open pit precedence and physical representation of the data.

Our basic underground model dataset consists of 1,123 development activities, 351 stoping activities and an equal number of backfilling activities. Stopes range from approximately 5,000 to 40,000 tonnes, resulting in 17 levels in the underground mine that are a maximum of 40 meters in height. The required development and backfilling is estimated based on the stope properties. Each activity has up to 12 immediate predecessors and up to 100 delay constraints. Subsection 2.2 provides a description of the underground mine's precedence structure. For our analysis, we construct ten distinct scenarios, each for a 24-year time horizon with decisions made at yearly fidelity, and each defined as a set of upper bounds on the resource constraints and a given discount rate (Table 1). We set the underground backfilling capacity equal to the underground extraction capacity.

Table 1: (Scenario Summary) Capacities and discount rates used in each scenario, with equation numbers from the enhanced transition model also given in the column headers.

Scenario	Annual Capacities				Annual Discount Rate
	Extraction		Development		
	Open Pit (t) (10l)	Underground (t) (10n)	(m) (10n)	Mill (t) (10m)	
1	50,000,000	2,000,000	5000	8,000,000	9%
2	50,000,000	2,000,000	5000	7,000,000	9%
3	50,000,000	2,000,000	2500	8,000,000	9%
4	50,000,000	1,500,000	5000	8,000,000	9%
5	40,000,000	2,000,000	5000	8,000,000	9%
6	40,000,000	2,000,000	5000	7,000,000	9%
7	50,000,000	2,000,000	5000	6,000,000	9%
8	50,000,000	1,500,000	2500	8,000,000	9%
9	50,000,000	2,000,000	5000	8,000,000	1%
10	50,000,000	2,000,000	5000	8,000,000	15 %

5.2. Numerical Results

We compare the performance of the OMP Solver (Muñoz et al., 2015) to that of AMPL/CPLEX, (IBM CPLEX Optimizer, 2014; AMPL Optimization LLC, 2014), using a Dell PowerEdge R410 with 16 processors (2.72 GHz each) and 28 GB of RAM. OMP, Version 1509 is an academic, customized solver that uses standard preprocessing and exploits the mathematical structure of PCPSP to solve the LP relaxation quickly using the BZ algorithm; then, we execute the TopoSort heuristic eleven times, each with a different alpha point value between 0 and 1, inclusive, incremented by 0.1; this procedure transforms the LP relaxation to an integer-feasible solution, of which we choose the best one. All other parameter settings are default. CPLEX 12.6.0.0 uses default parameter settings other than memory emphasis, and 40,000-second time limit. Variable elimination techniques are employed before passing the model to CPLEX (Lambert et al., 2014; O'Sullivan, 2013). Both solvers provide solutions to the enhanced transition model, ($\mathbb{T}^e$), with the same crown and sill pillar placement options available in each scenario. Depending on the crown and sill pillar placement, for our dataset, the enhanced transition model, ($\mathbb{T}^e$), averages 50,000 variables and 1.5 million constraints. (The numerical performance of ($\mathbb{T}^b$) is dominated by that of ($\mathbb{T}^e$) using our methodology; see Appendix.)

We first compare the performance using CPLEX to solve the enhanced transition model ($\mathbb{T}^e$) for a fixed crown and sill pillar location (giving CPLEX the benefit of the faster LP solver) against that of the OMP Solver. For a representative crown and sill pillar placement given as the ordered pair [(820), (460)], where these elevations are relative to sea level, the enhanced transition model, ($\mathbb{T}^e$), contains approximately 60,000 variables and 1,200,000 constraints, of which 120 are "side" constraints. CPLEX averages 163.77 seconds with the faster LP solver for each LP relaxation over the ten scenarios, and produces slightly better integer solutions in only two of the ten scenarios (while CPLEX is unable to find an integer-feasible solution in the other scenarios due either to memory or time limitations). By contrast, OMP is able to solve the LP relaxations in fewer than ten seconds, regardless of the scenario, and produces an integer solution within 6% of optimality or better in just a few additional seconds (Table 2).

Figure 7 depicts the LP relaxation objective function value and the best known IP objective function value for each reasonable set of crown and sill pillar placements for Scenario 1 using the OMP Solver. Both the LP relaxation objective function value and the best-known IP objective function value follow the same

Table 2: (OMP and CPLEX comparison) Comparison of solution times and optimality gaps between the OMP Solver and CPLEX for ($\mathbb{T}^e$) . All scenarios are run with a crown pillar located at elevation 820 and a sill pillar located at level 460.

Scenario	CPLEX				OMP Solver		
	LP Solution Time (sec)		IP Solution	Optimality	LP Solution	TopoSort Solution	Optimality
	Barrier	Simplex*	Time (sec)	Gap	Time (sec)	Time (sec)	Gap
1	163.75	488.41	†	—	9.72	3.59	2.78%
2	163.68	490.24	†	—	5.23	3.13	3.56%
3	177.85	1631.15	†	—	8.43	3.29	4.23%
4	183.08	577.07	‡	—	6.42	3.67	3.90%
5	146.24	613.93	26,100	2.66%	6.28	3.62	4.49%
6	172.88	783.70	34,728	2.67%	6.60	3.44	5.86%
7	152.41	416.32	‡	—	5.44	3.12	4.76 %
8	152.00	1300.20	‡	—	8.57	2.14	4.71%
9	163.26	707.38	†	—	4.80	2.41	0.64%
10	162.59	653.63	†	—	5.10	2.87	4.24%

*CPLEX is allowed to choose the variant of simplex to use, which results in employing dual simplex on the dual problem

† CPLEX was unable to produce an integer solution within a 5% gap before running out of memory

‡CPLEX was unable to produce an an integer solution within a 5% gap before the 40,000 second limit

Note: Optimality gaps are calculated as $100\% \cdot \left(1 - \left(\frac{\text{IP Obj. Func. Value}}{\text{LP Relaxation Value}}\right)\right)$

trend as we exhaustively enumerate all of the 3,500 crown and sill pillar placement options. The average gap between the LP relaxation objective function value and the best-known IP objective function value is, on average, 3.91%, and the time to obtain the integer solution is, on average, 9.78 seconds. This gap also appears to be relatively consistent across all of the crown and sill pillar placement options for this scenario. The LP relaxation with the largest objective function value produces the largest IP objective function value, suggesting empirically that our solution methodology provides consistently high-quality IP solutions relative to the LP solutions for the enhanced transition model, ($\mathbb{T}^e$).

Our ad-hoc branch-and-bound strategy supplies a wealth of information for the mine operator: Crown pillar placement affects the NPV significantly more than sill pillar placement. Additional insights might involve geology: if it is undesirable to have a crown pillar located at elevation 820, moving the crown pillar to elevation 780 would have the least impact on the mine's NPV (Figure 7).

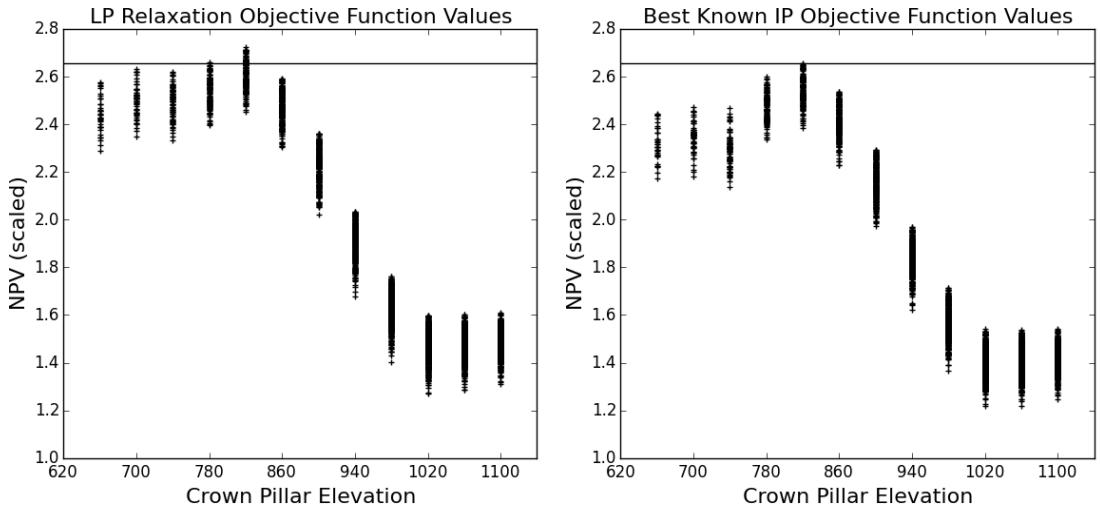

Figure 7: (LP and IP Comparison) Left: LP relaxation values for all feasible crown and sill pillar placement options. Right: Best-known IP objective function value for the corresponding crown and sill pillar placement options. The vertical band of crosses at each crown pillar elevation is associated with the scaled NPV corresponding to all viable sill pillar location combinations. A horizontal line indicates overall best-known IP objective function value for Scenario 1.

It is possible to heavily prune our ad-hoc branch-and-bound tree using *bound dominance*. For example, for Scenario 1, after we obtain an IP objective function value associated with the crown and sill pillar placement option that has the highest LP relaxation objective function value, we can eliminate solving the integer program corresponding to all crown and sill pillar placements whose LP relaxation objective function value is lower. Only 40 of the over 3,500 crown and sill pillar placement options have an LP relaxation objective function value greater than the best known IP objective function value (Figure 8). The mine planner interested in robust solutions might note that of those options, only one of them is not associated with a crown pillar located a elevation 820, and the corresponding LP relaxation's objective function value is only 0.13% greater than the best-known IP objective function value.

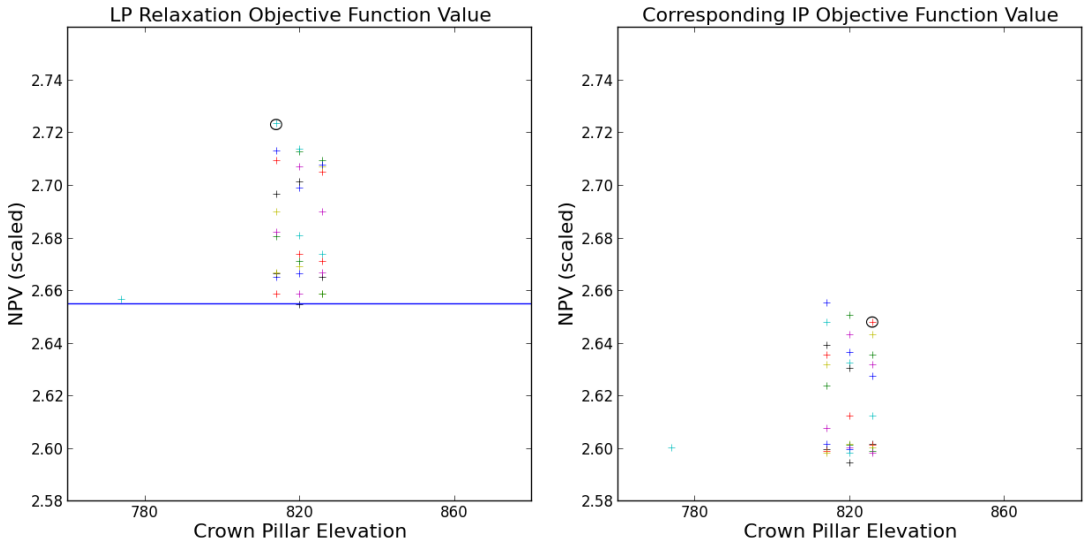

Figure 8: (Zoom Comparison) Left: LP relaxation values associated with crown and sill pillar placements that produce a high objective function relaxation value, and a horizontal line representing the best-known IP objective function value. Right: Corresponding IP objective function values for models whose LP relaxation objective function value is greater than the best known IP objective function value. Note: Circled is the best LP relaxation objective function value and its corresponding IP objective function value.

Table 3 summarizes the near optimal crown and sill pillar placement options associated with each scenario. The average gap between the LP and IP objective function values is 5.55%. For any scenario with a discount rate of 9%, the crown pillar associated with the highest IP objective function value is located at the same elevation, 820. (Changing the discount rate affects the best-known crown and sill pillar locations.) Techniques may be employed to reduce the gaps, but, for the scenarios we tested, it is unlikely that such refinements would lead to solutions with a change to the crown pillar placement, because of the 40 solutions not eliminated by bound dominance, only one had a placement at a level other than 820 (see Figure 8). We report solution time as the CPU time required to solve the LP relaxations associated with all reasonable crown and sill pillar placement options, plus that required to solve the necessary integer programs, i.e., those not excluded by bound dominance. However, our procedure is massively parallelizable in that all LPs can be solved simultaneously, as can all relevant IPs. Hence, on average, even the longest-running scenarios would require fewer than ten seconds to solve with the appropriate hardware; our methodology efficiently provides a way to identify near-optimal crown and sill pillar placements where no such methodology had existed.

Qualitatively, we can establish some generalities about the schedules for each scenario. The crown pillar

location that is chosen in a majority of the scenarios, 820, contains the fifth-highest amount of metal, and, as such, does not correspond to an intuitive solution of minimizing lost metal. Additionally, for the best schedule we report for each scenario, underground construction and production begins as soon as possible owing to that fact that all underground mine production is sufficiently high grade that it displaces material from the open pit at the mill. We do observe some fluctuations in both the open pit and underground production, which is undesirable from an operational standpoint, and would require smoothing to create an operationally feasible schedule. However, these fluctuations are not uncommon in a strategic plan.

Table 3: (Scenario Summary) Optimal solution, integrality gap, and total solution time for each scenario if enumerated crown and sill pillar placement solves are performed in serial.

Scenario Number	Optimal Crown and Sill Pillar Placement	Integrality Gap	Total Solution Time (sec)
1	[(820), (500)]	2.51%	29,652
2	[(820), (420)]	3.28%	28,220
3	[(820), (500)]	3.25%	30,642
4	[(820), (660)]	3.42%	31,426
5	[(820), (500)]	4.40%	25,993
6	[(820), (420)]	4.97%	27,404
7	[(820), (460)]	4.76%	36,312
8	[(820), (500)]	3.45%	41,652
9	[(700),(420)]	0.70%	26,016
10	[(820), (500,660)]	3.65%	23,825

Notes: Crown and sill pillar placement option format is [(Crown Pillar Elevation), (Sill Pillar Elevation(s))]
Total solution time is the time required for the LPs associated with all possible crown and sill pillar locations, and the additional time to obtain an IP solution for the non-dominated LP relaxations.

6. Conclusions and Future Work

The methodology developed in this paper provides a robust framework for solving a linear-integer program representing an open-pit-to-underground transition model involving scenarios that contain 50,000 variables and over 1.5 million constraints. An ad-hoc branch-and-bound scheme fixes the variables that destroy the PCPSP structure without compromising optimality. This methodology permits us to test a wide variety of scenarios quickly and provides a better understanding of how crown and sill pillar placement affects NPV.

With our specialized technique, we are able to solve a relevant and economically significant problem for the mining industry. As current open pit mines are required to extract an increasing number of tons of waste material for every ton of ore, it becomes crucial to identify the proper transition location. Although, for confidentiality reasons, the exact NPVs are not given, our results show that the NPV can change by

hundreds of millions of dollars depending on the crown pillar placement, and by tens of millions based on the sill pillar placement. Our model provides not only a near-optimal solution, but identifies the economic outcome of all possible crown and sill pillar placements.

Many mine operators defer underground mining until the open pit has finished production, resulting in insufficient cash flow to justify an underground mine and an unmined portion of the deposit that could have been extracted economically. By developing an efficient and tractable solution methodology, we can provide mine operators with a tool to better understand the benefits of each transition elevation, and the ability to confidently make a timely decision.

Additional work could address: (i) accuracy, (ii) applicability, and (iii) optimality gap. The accuracy of the model would be improved with a better representation of the stockpiles. Since stockpiles contribute significantly to the NPV, it would be beneficial to include mixing of ore in the stockpile and the degradation of ore grade over time. The applicability of the model could be improved by adding blending requirements at the mill and non-zero lower bounds on the knapsack constraints, which can be vital to maintain proper mill feed, but that would destroy the mathematical structure that the TopoSort heuristic relies on. Finally, we wish to incorporate a branch-and-bound algorithm within the OMP Solver to reduce the optimality gap for a fixed crown and sill pillar placement option.

7. Acknowledgments

Alexandra Newman and Barry King received funding from the Center for Innovation in Earth Science and Engineering at the Colorado School of Mines, and from Alford Mining Systems. Marcos Goycoolea received funding from FONDECYT grant #1151098 and CONICYT PIA Anillo grant 1407. The authors acknowledge Monica Dodd, Chris Alford, Xiaolin Wu, Hongliang Wang, Ralf Kintzel, Conor Meagher, and many others for their continued support of and advocacy for this project. This research benefited significantly from suggestions made by Daniel Espinoza (Universidad de Chile), Eduardo Moreno (Universidad Adolfo Ibañez), Orlando Rivera (Universidad Adolfo Ibañez), and Andrea Brickey (South Dakota School of Mines).

C. Alford. Optimisation in underground mining. In *Handbook of Operations Research in Natural Resources*. 2007.

C. Alford. *Optimization in underground mine design*. PhD thesis, University of Melbourne, 2006.

A. Alonso-Ayuso, F. Carvallo, L.F. Escudero, M. Guignard, J. Pi, R. Puranmalka, and A. Weintraub. Medium range optimization of copper extraction planning under uncertainty in future copper prices. *European Journal of Operational Research*, 233(3):711–726, 2014.

AMPL Optimization LLC. *Version 20140908*, 2014. www.ampl.com.

O. Araneda. *Opportunities and Challenges of the Transition from an Open Pit to an Underground Operation in the Chuquicamata Mine*. Presentation, Mine Planning 2015, Antofagasta, Chile, 2015.

M. Ataee-Pour. *A Heuristic Algorithm to Optimise Stope Boundaries*. PhD thesis, University of Wollongong, 2000.

E. Bakhtavar, K. Shahriar, and K. Oraee. A model for determining the optimal transition depth over from open-pit to underground mining. 5th International Conference and Exhibition on Mass Mining, 2008.

D. Bienstock and M. Zuckerberg. Solving LP relaxations of large-scale precedence constrained problems. *Integer Programming and Combinatorial Optimization*, 6080(1):1–14, 2010.

A. Bley, N. Boland, G. Froyland, and M. Zuckerberg. Solving mixed integer nonlinear programming problems for mine production planning with stockpiling. *Optimization Online*, Preprint:1–30, 2012.

M. Brazil and D.A. Thomas. Network optimization for the design of underground mines. *Networks*, 49(1): 40–50, 2007.

A. Brickey. *Underground production scheduling optimization with ventilation constraints*. PhD thesis, Colorado School of Mines, 2015.

M. Carlyle and C. Eaves. Underground planning at Stillwater Mining Company. *Interfaces*, 31(4):50–60, 2001.

R. Chicoisne, D. Espinoza, M. Goycoolea, E. Moreno, and E. Rubio. A new algorithm for the open-pit mine production scheduling problem. *Operations Research*, 60(3):517–528, 2012.

J. Crawford and W. Hustrulid. *Open Pit Mine Planning and Design*. Society of Mining Engineers, 1st edition, 1979.

R. Epstein, M. Goic, A. Weintraub, J. Catalàn, P. Santibáñez, R. Urrutia, R. Cancino, S. Gaete, A. Aguayo, and F. Caro. Optimizing long-term production plans in underground and open-pit copper mines. *Operations Research*, 60(1):4–17, 2014.

A. Finch. Open pit to underground. *International Mining*, January:88–89, 2012.

M.E. Gershon. Mine scheduling optimization with mixed integer programming. *Min. Eng. (Littleton, Colo.)*, 35(4):351–354, 1983.

H. Hamrin. *Guide to Underground Mining Methods and Applications*. Atlas Copco, 1st edition, 1997.

IBM CPLEX Optimizer. *Version 12.4.0.0.* 2013. http://www-01.ibm.com/software/commerce/optimization/cplex-optimizer/.

T. Johnson. Optimum open pit mine production scheduling. Technical report, University of California, Berkeley, 1968.

B. Lambert, A. Brickey, A. Newman, and K. Eurek. Open pit sequencing formulations: A tutorial. *Interfaces*, 62(3):127–142, 2014.

H. Lerchs and Grossman. Optimum design of open-pit mines. *Canadian Institute of Mining Bulletin*, 58: 47–54, 1965.

M. Martinez, and A. Newman. A solution approach for optimizing long- and short-term production scheduling at LKABs Kiruna mine. *European Journal of Operational Research*, 211(1):184–197, 2011.

Minemax. *Mine Planning and Scheduling Solutions*. 2013. www.minemax.com.

E. Moreno, M. Rezakhah, A. Newman, and F. Ferreira. Linear models for stockpiling in open-pit mining production scheduling problems. *Working Paper*, 2016.

G. Muñoz, D. Espinoza, M. Goycoolea, E. Moreno, M. Queyranne, and O. Rivera. Production scheduling for strategic open pit mine planning, part I: A mixed integer programming approach. *Working Paper*, 2015.

A. Newman, and M. Kuchta. Using aggregation to optimize long-term production planning at an underground mine. *European Journal of Operational Research*, 176(2):1205–1217, 2007.

A. Newman, E. Rubio, R. Caro, and A. Weintraub. A review of operations research in mine planning. *Interfaces*, 40(3):222–245, 2010.

A. Newman, C. A. Yano, and E. Rubio. Mining above and below gorund: Timing the transition. *IIE Transactions*, 45(8):865–882, 2013.

M. Osanlo, J. Gholamnejed, and B. Karimi. Long-term open pit mine production planning: a review of models and algorithms. *International Journal of Mining, Reclamation, and Environment*, 22(1):3–35, 2008.

D. O'Sullivan. *An optimization-based decomposition heuristic for solving complex underground mine scheduling problems*. PhD thesis, Colorado School of Mines, 2013.

D. O'Sullivan, and A. Newman. *Optimization-based heuristics for underground mine scheduling*. *European Journal of Operational Research*, 241(1):248–259, 2015.

J. Picard. Maximal closure of a graph and applications to combinatorial problems. *Management Science*, 22 (11):1268–1272, 1976.

C. Qinglin, B. Stillborg, and C. Li. Optimisation of undergound mining methods using grey theory and nerual networks. Balkema, Rotterdam, 1996. Mine Planning and Equipment Selection Conference.

S. Ramazan. The new fundamental tree algorithm for production scheduling of open pit mines. *European Journal of Operational Research*, 177(2):1153–1166, 2007.

M. S. Shishvan, and J. Sattarvand. Long term production planning of open pit mines be any colony optimization. *European Journal of Operational Research*, 240(3):825–836, 2015.

J. F. Souza, I. M. Coelho, S. Ribas, H. .G Santos, and L. H. C. Merschmann. A hybrid heuristic algorithm for the open-pit-mining operational planning problem. *European Journal of Operational Research*, 207(2):1041–1051, 2010.

E. Topal, and S. Ramazan. A new MIP model for mine equipment scheduling by minimizing maintenance cost. *European Journal of Operational Research*, 207(2):1065–1071, 2010.

L. Trout. *Formulation and Application of New Underground Mine Scheduling Models*. PhD thesis, The University of Queensland, 1997.

R. Underwood, and B. Tolwinski. A mathematical programming viewpoint for solving the ultimate pit problem *European Journal of Operational Research*, 107(1):96–107, 1998.

Whittle Consulting. Whittle consulting global optimization software, 2013. http://www.whittleconsulting.com.au/.

8. Appendix

We demonstrate here computationally that, for the scenarios we examine, the LP relaxation of the basic transition model ($\mathbb{T}^b$) is weak relative to that of the enhanced transition model ($\mathbb{T}^e$), and we compare LP solution times across standard algorithms. We also show that CPLEX is unable to solve the basic transition model ($\mathbb{T}^b$) for any scenario, i.e., that the basic transition model is intractable when solved with CPLEX. Furthermore, two proofs – one each for the special knapsack and inventory balance constraints (see §3) – show that our reformulations are no weaker than the original ones; moreover, computational results show that the reformulations are strictly stronger.

8.1. Solutions to the Basic Transition Model ($\mathbb{T}^b$)

Table 4 provides specific information regarding algorithmic performance and solution quality for our ten test scenarios. We first compare solution times for standard LP algorithms when used to solve ($\mathbb{T}^b$). All computations were run on the same server as the enhanced transition model ($\mathbb{T}^e$). The barrier outperforms the best version of simplex in all cases; the academic nature of the OMP Solver precludes it from handling the complexity in the basic transition model, ($\mathbb{T}^b$), in particular, the decisions regarding crown and sill pillar placement (hence, our ad-hoc branch-and-bound strategy). Despite the ability of CPLEX (Version 12.6.0.0 using default parameter settings other than turning on memory emphasis) to solve the LP relaxation of ($\mathbb{T}^b$), the complexity of the problem proves intractable when seeking a good, integer-feasible solution. For all our scenarios, CPLEX exhausts a 40,000-second time limit or runs out of memory before a solution within 5% of optimality is found. We attribute this poor performance, in part, to the weak LP bound (as seen with a comparison of the scaled net present values in the penultimate and last columns of Table 4). By contrast, the results we obtain from using our reformulations and solution procedure on ($\mathbb{T}^e$) result not only in tighter bounds, but also in near-optimal integer solutions, the latter stemming in large part from the the mathematical structure of ($\mathbb{T}^e$) our TopoSort heuristic is able to exploit. The values for the tight LP relaxation solution we obtain from ($\mathbb{T}^e$) in Table 4 result from the fixed crown and sill pillar combination that gives the best objective function value for that scenario.

Table 4: (Basic and Enhanced Comparison) Comparison of solution times and solutions gaps between the basic transition model ($\mathbb{T}^b$) and the enhanced transition model ($\mathbb{T}^e$) using CPLEX.

Scenario	LP Solution Time for ($\mathbb{T}^b$) (sec)		IP Solution	($\mathbb{T}^b$) LP	Largest ($\mathbb{T}^e$)
	Barrier	Simplex*	Time (sec)	Value	LP Value
1	373.98	10343.09	†	3.20	2.72
2	359.53	8222.94	†	3.11	2.66
3	992.07	13821.83	‡	2.71	2.55
4	333.09	13163.29	‡	3.11	2.70
5	300.37	7451.82	†	3.20	2.70
6	338.96	8018.63	†	3.09	2.64
7	407.66	7792.96	†	3.01	2.58
8	756.81	25526.81	‡	2.71	2.55
9	383.78	8240.55	‡	6.24	4.86
10	369.52	7738.03	†	2.19	2.06

*CPLEX is allowed to choose the variant of simplex to use, which results in employing dual simplex on the dual problem
† CPLEX was unable to produce an integer solution within 5% gap before running out of memory
‡CPLEX was unable to produce an an integer solution within 5% gap before the 40,000 second limit of the LP relaxation before running out of memory

8.2. On the strength of the Special Knapsack reformulation

In this section, we prove that the reformulation of the special knapsack constraints (1j), presented in Section 3.1, is not weaker than the original formulation.

For simplicity, but without loss of generality, we consider the case of a single phase. For notation purposes, assume that the blocks in the phase are numbered $1, \ldots, |\mathcal{B}|$ and that there is a limit of k blocks that can be extracted in a given time period. (In Section 3.1, this term is represented as $\bar{r}$). We assume variables x_{bt} are defined as before:

$$x_{bt} = \begin{cases} 1 & \text{if block } b \text{ is extracted by time } t \\ 0 & \text{otherwise.} \end{cases}$$

We can model the bound of k extractable blocks in a time period either by adding the knapsack constraint:

$$\sum_{b=1}^{|\mathcal{B}|} (x_{bt} - x_{b,t-1}) \leq k, \forall t \in \mathcal{T} \ni t > 1 \tag{11}$$

or by adding precedence constraints:

$$x_{bt} \leq x_{b-k,t-1} \qquad \forall b \in \mathcal{B} \ni b \geq k+1, t \in \mathcal{T} \ni t > 1. \tag{12}$$

We now show that (12) is at least as strong as (11).

Lemma Let $\mathcal{X}$ be the set of x_{bt} variables such that:

$$x_{bt} \leq x_{b-1,t} \quad \forall t, b \in \mathcal{B} \ni b \geq 1 \tag{13a}$$

$$x_{bt} \leq x_{b,t+1} \quad \forall b \in \mathcal{B}, t \leq |\mathcal{T}| - 1 \tag{13b}$$

$$0 \leq x_{bt} \leq 1 \qquad \forall b \in \mathcal{B}, t \in \mathcal{T}. \tag{13c}$$

For sets:

$$\mathcal{P}_1 = \{x \in \mathcal{X} : \sum_{b=1}^{|\mathcal{B}|} (x_{bt} - x_{b,t-1}) \leq k \quad \forall t \in \mathcal{T}\}$$

$$\mathcal{P}_2 = \{x \in \mathcal{X} : x_{bt} \leq x_{b-k,t-1} \quad \forall b \in \mathcal{B} \ni b \geq k+1, \quad \forall t \in \mathcal{T}\}$$

we wish to show that $\mathcal{P}_2 \subseteq \mathcal{P}_1$.

Proof.

We show that if x_{bt} satisfies (12), then x_{bt} satisfies (11). For each $t \in \mathcal{T}$:

$$\begin{aligned}
\sum_{b=1}^{|\mathcal{B}|} (x_{bt} - x_{b,t-1}) &= \sum_{b=1}^{k} x_{bt} - \sum_{b=1}^{|\mathcal{B}|-k} x_{b,t-1} + \sum_{b=k+1}^{|\mathcal{B}|} x_{bt} - \sum_{b=|\mathcal{B}|-k+1}^{|\mathcal{B}|} x_{b,t-1} \\
&\leq \sum_{b=1}^{k} x_{bt} - \sum_{b=1}^{|\mathcal{B}|-k} x_{b,t-1} + \sum_{b=k+1}^{|\mathcal{B}|} x_{b-k,t-1} - \sum_{b=|\mathcal{B}|-k+1}^{|\mathcal{B}|} x_{b,t-1} \\
&= \sum_{b=1}^{k} x_{bt} - \sum_{b=1}^{|\mathcal{B}|-k} x_{b,t-1} + \sum_{b=1}^{|\mathcal{B}|-k} x_{b,t-1} - \sum_{b=|\mathcal{B}|-k+1}^{|\mathcal{B}|} x_{b,t-1} \\
&= \sum_{b=1}^{k} x_{bt} - \sum_{b=|\mathcal{B}|-k+1}^{|\mathcal{B}|} x_{b,t-1} \\
&\leq \sum_{b=1}^{k} x_{bt} \\
&\leq k \quad \blacksquare
\end{aligned}$$

Combining the first and last expressions implies that $\sum_{b=1}^{|\mathcal{B}|} (x_{bt} - x_{b,t-1}) \leq k$. The reformulation of the special knapsack constraints is done not only to enable the model to be more easily solved within a framework the OMP Solver can handle, but also to improve the upper bound. For ($\mathbb{S}$), the reformulation does not improve the LP solution time over that obtained with the original model when using the OMP Solver for

both formulations; however, for the scenarios we test, the LP bound for ($\mathbb{S}$) improves with the reformulation by approximately 10%.

8.3. Inventory Balance Reformulation as Variable Substitution

In this subsection, we show that the reformulation of the inventory balance constraints (6) and the corresponding variable substitutions into expressions (7)-(9) presented in Section 3.2, is not weaker than the original formulation. To this end, it suffices to show that for every integer-feasible solution of the reformulation, there exists a corresponding feasible solution to the original formulation having the same objective function value. Given a solution $\hat{Y}^{\mathbb{S}}_{bt}, Z^{\mathbb{S}}_{nbt}$ of the reformulation, we construct a feasible solution in the original space via the following linear mapping:

$$
\begin{aligned}
I^{\mathbb{S}}_{nbt} &= \hat{Y}^{\mathbb{S}}_{b,t-1} - Z^{\mathbb{S}}_{nb,t-1} \quad \forall b \in \mathcal{B}, n \in \mathcal{N}_b, t \in \mathcal{T} \\
I^{\mathbb{S}-}_{nbt} &= Z^{S}_{nbt} - Z^{\mathbb{S}}_{nb,t-1} \quad \forall b \in \mathcal{B}, n \in \mathcal{N}_b, t \in \mathcal{T} \\
Y^{\mathbb{S}}_{nb2t} &= \hat{Y}^{\mathbb{S}}_{bt} \quad \forall b \in \mathcal{B}, n \in \mathcal{N}_b, t \in \mathcal{T} \\
Y^{\mathbb{S}}_{nb1t} &= 0 \quad \forall b \in \mathcal{B}, n \in \mathcal{N}_b, t \in \mathcal{T} \\
Y^{\mathbb{S}}_{nb3t} &= 0 \quad \forall b \in \mathcal{B}, n \in \mathcal{N}_b, t \in \mathcal{T}
\end{aligned}
$$

That is, substituting into ($\mathbb{S}$) the expressions on the right-hand-side of the mapping for the variables listed on the left-hand side results in true statements for each relevant set of constraints. (Constraints containing only variables not involved in the mapping remain unchanged.) This implies that the solution involving $\hat{Y}^{\mathbb{S}}_{bt}$ and$Z^{\mathbb{S}}_{nbt}$ is feasible, and therefore valid, for ($\mathbb{S}$). The same type of substitution, and the correct interpretation of the new variables $\hat{Y}^{\mathbb{S}}_{bt}$ and $Z^{\mathbb{S}}_{nbt}$ yeilds the same objective function value as in the original formulation.